THE JOURNAL OF BIOLOGICAL CHEMISTRY VOL. 284, NO. 50, pp. 34628–34639, December 11, 2009

Sunday Driver Interacts with Two Distinct Classes of Axonal Organelles*[S]◆

Received for publication, June 17, 2009, and in revised form, September 25, 2009 Published, JBC Papers in Press, September 29, 2009, DOI 10.1074/jbc.M109.035022

Namiko Abe[‡], Angels Almenar-Queralt[§], Concepcion Lillo[¶1], Zhouxin Shen[‖], Jean Lozach[§], Steven P. Briggs[‖], David S. Williams[¶2], Lawrence S. B. Goldstein[§], and Valeria Cavalli[‡3]**

*From the [‡]Department of Anatomy and Neurobiology, Washington University in St. Louis, St. Louis, Missouri 63110, the [§]Department of Cellular and Molecular Medicine, Howard Hughes Medical Institute, the [¶]Departments of Pharmacology and Neurosciences, and the [‖]Section of Cell and Developmental Biology, Division of Biological Sciences, University of California, San Diego, La Jolla, California 92093, and the **Departments of Ophthalmology and Neurosciences, Jules Stein Eye Institute, UCLA, Los Angeles, California 90095*

The extreme polarized morphology of neurons poses a challenging problem for intracellular trafficking pathways. The distant synaptic terminals must communicate via axonal transport with the cell soma for neuronal survival, function, and repair. Multiple classes of organelles transported along axons may establish and maintain the polarized morphology of neurons, as well as control signaling and neuronal responses to extracellular cues such as neurotrophic or stress factors. We reported previously that the motor-binding protein Sunday Driver (syd), also known as JIP3 or JSAP1, links vesicular axonal transport to injury signaling. To better understand syd function in axonal transport and in the response of neurons to injury, we developed a purification strategy based on anti-syd antibodies conjugated to magnetic beads to identify syd-associated axonal vesicles. Electron microscopy analyses revealed two classes of syd-associated vesicles of distinct morphology. To identify the molecular anatomy of syd vesicles, we determined their protein composition by mass spectrometry. Gene Ontology analyses of each vesicle protein content revealed their unique identity and indicated that one class of syd vesicles belongs to the endocytic pathway, whereas another may belong to an anterogradely transported vesicle pool. To validate these findings, we examined the transport and localization of components of syd vesicles within axons of mouse sciatic nerve. Together, our results lead us to propose that endocytic syd vesicles function in part to carry injury signals back to the cell body, whereas anterograde syd vesicles may play a role in axonal outgrowth and guidance.

The length of axons often exceeds by several orders of magnitude the dimension of the neuronal cell body. Protein complexes and vesicles must travel long distances to establish and then maintain proper connections between neuronal cell bodies and their targets. Dysfunction of proteins involved in axonal transport has been recently linked to neurodegenerative diseases, revealing a role of axonal transport in neuronal function (1, 2). Although the role of molecular motors in axonal transport is now well established, we know little about the nature of the organelles moving in axons and the machinery regulating their transport.

Although synaptic vesicles are well characterized trafficking organelles (3–7), to date, few attempts to purify and characterize axonally transported vesicular compartments at the morphological and biochemical level have been carried out. These include dense-core granulated vesicles transporting the presynaptic active zone components Piccolo and Bassoon to nascent synapses (8) and retrograde signaling endosomes (9–11). The observation that both endosomal markers Rab5 (10) and Rab7 (11) contribute to retrograde axonal transport of neurotrophins indicates that both early and late endosomes regulate neurotrophin signaling. The axonal transport of multiple classes of endosomes may provide precise control of the strength, duration, and localization of neurotrophic signaling as well as the response to other extracellular cues such as stress or injury. In addition, distinct classes of endosomes and other organelles may establish and maintain the extreme polarized morphology of neurons.

The recruitment of motor proteins to endosomes has been characterized in non-neuronal cells (12), but it remains to be determined whether similar mechanisms exist in neurons. One potential motor adaptor on axonal endosomes is Sunday Driver (syd), also known as JIP3 (or JSAP1) (13–15). syd interacts with the anterograde motor kinesin-I (13) and with the retrograde motor complex dynein-dynactin (16). In peripheral nerves, syd associates with both anterograde and retrograde vesicles of distinct size and morphology (16). In response to nerve injury, syd preferentially interacts with dynactin, resulting in a net increase in retrograde transport of the signaling molecule JNK[4] (16). syd

* This work was supported, in whole or in part, by NINDS National Institutes of Health Grant R01 NS060709 (to V. C.) and NIGMS National Institutes of Health Grant GM35252 (to L. S. B. G.) and NEI National Institutes of Health Grant EY07042 (to D. S. W.). This work was also supported by National Science Foundation Grant IBN 0619411 (to S. P. B.).
◆ This article was selected as a Paper of the Week.
[S] The on-line version of this article (available at http://www.jbc.org) contains six supplemental tables (supplemental Data S1–S6).
[1] Present address: Instituto de Neurociencias de Castilla y León, 37007 Salamanca, Spain.
[2] A Jules and Doris Stein Research to Prevent Blindness Professor.
[3] To whom correspondence should be addressed: Dept. of Anatomy and Neurobiology, Washington University School of Medicine, Campus Box 8108, 660 S. Euclid Ave., St. Louis, MO 63110-1093. Tel.: 314-362-3540; Fax: 314-362-3446; E-mail: cavalli@pcg.wustl.edu.

[4] The abbreviations used are: JNK, c-Jun NH_2-terminal kinase; MAPK, mitogen-activated protein kinase; VAMP, vesicle-associated membrane protein; MVB, multivesicular bodies; PBS, phosphate-buffered saline; BSA, bovine serum albumin; LC-MS/MS, liquid chromatography tandem mass spectrometry; EM, electron microscopy; SVP, small vesicle pool; LVP, large vesicle pool.

may thus mediate the axonal transport of vesicles, which function as mobile signaling platforms to convey information about axonal injury back to the cell body. In addition, syd-dependent vesicular transport may be critical for axonal growth and regeneration because syd deletion in the central nervous system results in axonal outgrowth defects (17, 18).

Retrograde injury signals traveling from the injury site back to the cell body are essential to increase the intrinsic growth capacity of neurons following injury and promote successful regeneration (19–22). Although syd-dependent vesicular transport may represent one mechanism by which axons respond to injury, several distinct injury-signaling pathways have been recently characterized. Activation of mitogen-activated protein kinases (MAPKs), such as JNK (16) and in particular extracellular signal-regulated kinase (Erk), and its interaction with the dynein-dynactin retrograde molecular motors are required for regeneration (16, 23). In addition to MAPKs, axonal injury activates transcription factors, including STAT3, through the local release of cytokines (19). Axons also use mRNA translation to transfer injury signals to the nucleus of injured neurons. Axonal mRNA translation and *de novo* synthesis of proteins such as importin-β (24) and vimentin (25) link the nuclear import machinery to retrograde injury signaling. The large population of mRNAs localized to sensory axons (25) indicates that sensory axons have the potential to respond to injury by synthesizing a complex population of proteins. Sumoylation might serve as a mechanism to target axonal proteins for retrograde transport following injury as transport directionality of the RNA-binding protein La in axons is determined by sumoylation (26). Coordination between several injury-signaling pathways may serve as an indicator of the extent and nature of damage.

Understanding the nature of syd axonal vesicles may thus contribute to the definition of the mechanisms by which neurons initiate the appropriate regenerative program and control axonal outgrowth following injury. To identify new mechanisms and molecules that regulate the vesicular transport of signals along axons, we developed a biochemical purification strategy based on anti-syd antibodies conjugated to magnetic beads. This approach allowed us to determine the morphology and molecular identity of two distinct classes of syd-associated vesicles. Here we present evidence that one class of syd-associated vesicles belongs to the endocytic pathway, whereas another class of syd vesicles may play a role in axonal growth and guidance.

EXPERIMENTAL PROCEDURES

Antibodies and Reagents—syd antibodies were previously described (13). The antibodies are as follows: anti-p150^{Glued} (BD Biosciences), anti-JNK3 (Upstate Biotechnology), anti-kinesin heavy chain (KIF5C (28)), anti-tubulin DM1A (Sigma), anti-amyloid precursor protein (Chemicon), anti-syntaxin 13, anti-synaptophysin, anti-SNAP29, anti-synaptotagmin VII, anti-Rab5 and anti-cellubrevin/VAMP3 (Synaptic Systems), anti-myelin basic protein (Dako), anti-syntaxin, anti-synaptotagmin, anti-VAMP/synaptobrevin and anti-SNAP25 (StressGen), anti-COX4 (Clontech), secondary Alexa Fluor-labeled antibodies and Texas Red dextran 3000 MW (Molecular Probes), Na^+/K^+ (Upstate Biotechnology), anti-KIF3A (Covance), and anti-clathrin and anti-Rab11 (BD Biosciences). Dynabeads M450 and M500 were purchased from Dynal Biotech (Invitrogen). Secondary antibodies for immunoisolation, goat anti-rabbit IgG, and rabbit anti-mouse IgG were from Biodesign.

Subcellular Fractionation—Synaptosomal fractions were prepared from mouse cortices according to Ref. 29 with minor modifications (see Fig. 1*A*). Five brain cortices were homogenized in a glass-Teflon homogenizer at 512 rpm in 10 volumes of cold buffer B (0.32 M sucrose, 4 mM Hepes, pH 7.3, and protease and phosphatase inhibitors). After a 10-min spin at 800 × *g*, we obtained fractions P1 + S1. S1 was centrifuged 15 min at 9,200 × *g* to obtain S2 and P2, which is the crude synaptosome pellet. P2 was resuspended in 10 ml of B buffer and centrifuged 15 min at 10,500 rpm to give P2′, the washed crude synaptosome fraction. P2′ was then submitted to hypotonic shock by resuspending gently the P2′ pellet with 1 ml of B buffer and adding 9 ml of cold water and HEPES/NaOH, pH 7.2, 1 M to obtain a final concentration of 4 mM. Following a 30-min incubation on ice, the LS1 fraction enriched with synaptic vesicles was obtained by centrifugation for 20 min at 25,000 × *g*. The LP2 fraction was obtained by sedimentation of LS1 on a 38% sucrose cushion for 2 h at 165,000 × *g*. The LP2 fraction floating on top of the 38% cushion was collected and diluted four times in Hepes 4 mM, homogenized by eight strokes using a 24-gauge syringe, and loaded on top of a 10–38% continuous sucrose gradient. Following centrifugation for 4 h at 24,900 rpm (Beckman SW41), 12 fractions of 1 ml each were collected from top to bottom. Fractions 3 and 4 contain synaptic vesicles, and fractions 8, 9, and 10 contain presynaptic plasma membrane and endosomal markers.

Immunoisolation—Tosyl chloride activated M500 or M450 Dynabeads (Dynal Biotech/Invitrogen) were coated with secondary antibody according to the manufacturer's instructions. Beads were then washed in binding buffer (PBS BSA 0.1%, 2 mM EDTA), incubated 1–6 h at 4 °C with the primary antibody or negative control (preimmune serum or irrelevant antibody), and washed three times with PBS/BSA. 10 and 100 μg of starting fractions small vesicle pool (SVP) or large vesicle pool (LVP), respectively, were used for vesicle immunoisolation. SVP or LVP collected directly from the gradient were diluted in 5 volumes of PBS/BSA and incubated with coated magnetic beads overnight at 4 °C on a rotating wheel. Beads were washed 2 × 10 min with PBS/BSA and four times with PBS. Bound material was eluted by boiling beads in non-reducing sample buffer for 1 min and analyzed by Western blot.

EM Analyses—Isolated vesicle fractions or magnetic beads after immunoisolation and their respective control fractions were fixed with 2% paraformaldehyde, 2% glutaraldehyde in 0.1 M cacodylate buffer for 30 min. Samples were centrifuged in a pellet after fixation and rinsed in buffer. Later, pellets were rapidly embedded in warm 2% agar that was solidified on ice. The small blocks of pellets in agar were then postfixed in osmium and processed for embedding in Epon 812 resin. Ultrathin sections were mounted on copper grids and stained with uranyl acetate and lead citrate.

Mass Spectrometry Analyses—Proteins were eluted from beads by boiling in 50 ml of 2% (weight/volume) RapiGest

(Waters) prepared in 100 mM NaCl, 1 mM EDTA, and 50 mM Tris, pH 7.0, for 1 min. Beads were spun down, and supernatants were taken for trypsin digestion. Protein solutions were diluted four times by adding 150 μl of 10 mM Tris buffer (pH = 7.2). Proteins were reduced and alkylated using 2 mM Tris(2-carboxyethyl) phosphine (Fisher, AC36383) at 37 °C for 30 min and 5 mM iodoacetamide (Fisher, AC12227) at 37 °C for 30 min in darkness, respectively. The proteins were digested with 1 μg of trypsin (Roche Applied Science, 03 708 969 001) at 37 °C overnight. 1 μl of concentrated hydrochloric acid was added to each sample to precipitate RapiGest (pH = 2). Samples were incubated at 4 °C overnight and then centrifuged at 16,100 × *g* for 15 min. Supernatant was collected and centrifuged through a 0.22-μm filter and was ready for LC-MS/MS analysis.

Automated two-dimensional nanoflow LC-MS/MS analysis was performed using LTQ tandem mass spectrometer (Thermo Electron Corp.) employing automated data-dependent acquisition. An Agilent 1100 high pressure liquid chromatography system (Agilent Technologies, Wilmington, DE) was used to deliver a flow rate of 300 nl min^{-1} to the mass spectrometer through a splitter. Chromatographic separation was accomplished using a three-phase capillary column. Using an in-house constructed pressure cell, 5 μm of Zorbax SB-C18 (Agilent Technologies) packing material was packed into a fused silica capillary tubing (200-μm inner diameter, 360-μm outer diameter, 20 cm long) to form the first dimension RP column (RP1). A similar column (200-μm inner diameter, 5 cm long) packed with 5 μm of PolySulfoethyl (PolyLC) packing material was used as the SCX column. A zero dead volume 1-μm filter (IDEX Health & Science, M548) was attached to the exit of each column for column packing and connecting. A fused silica capillary (100-μm inner diameter, 360-μm outer diameter, 20 cm long) packed with 5 μm of Zorbax SB-C18 (Agilent Technologies) packing material was used as the analytical column (RP2). One end of the fused silica tubing was pulled to a sharp tip with the inner diameter smaller than 1 μm using a laser puller (Sutter P-2000) as the electrospray tip. The peptide mixtures were loaded onto the RP1 column using the same in-house pressure cell. To avoid sample carryover and keep good reproducibility, a new set of three columns with the same length was used for each sample. Peptides were first eluted from RP1 column to SCX column using a 0–80% acetonitrile gradient for 150 min. The peptides were fractionated by the SCX column using a series of eight-step salt gradients (0 mM, 30 mM, 60 mM, 100 mM, 1 M ammonium acetate for 20 min) followed by high resolution reverse phase separation using an acetonitrile gradient of 0–80% for 120 min.

The mass spectrometer was operated in positive ion mode with a source temperature of 150 °C and a spray voltage of 1500 V. Data-dependent analysis and gas phase separation were employed. The full MS scan range of 300–2000 *m*/*z* was divided into three smaller scan ranges (300–800, 800–1100, and 1100–2000 Da) to improve the dynamic range. Each MS scan was followed by four MS/MS scans of the most intense ions from the parent MS scan. A dynamic exclusion of 1 min was used to improve the duty cycle of MS/MS scans. About 100,000 MS/MS spectra were collected for each sample.

TABLE 1
Filtering criteria for autovalidation of database search results

Mode	Protein score	1+ peptide	2+ peptide	3+ peptide
Protein details	>20	>9, >50%	>9, >50%	>11, >50%
Peptide	NA[a]	>13, >50%	>13, >50%	>15, >50%

[a] NA, not applicable.

Raw data were extracted and searched using Spectrum Mill (Agilent Technologies, version A.03.02). MS/MS spectra with a sequence tag length of 1 or less were considered as poor spectra and discarded. The rest of the MS/MS spectra were searched against the International Protein Index (IPI) data base limited to mouse taxonomy (version 3.14, 68,632 protein sequences). The enzyme parameter was limited to full tryptic peptides with a maximum miscleavage of 1. All other search parameters were set to the Spectrum Mill default settings (carbamidomethylation of cysteines, ± 2.5 Da for precursor ions, ± 0.7 Da for fragment ions, and a minimum matched peak intensity of 50%). Search results for individual spectra were automatically validated using the filtering criteria listed in Table 1. A concatenated forward-reverse data base is used to calculate the *in situ* identification false discovery rates. The total number of protein sequences in the combined data base is 137,264. The false discovery rates of our identified proteins are 0.8% at the protein level. Proteins that share common peptides were grouped to address the data base redundancy issue. The proteins within the same group shared the same set or subset of unique peptides.

Spectra counting, *i.e.* number of peaks detected for a particular protein, was used as a semiquantitative method to determine the presence of proteins in each sample. Each immunoisolation experiment was performed twice, and the total spectra count was used as a relative measure of protein abundance in each category. Comparison of synaptic vesicle immunoisolation with the previously established synaptic vesicle protein composition (3) was used to define the threshold in spectra counts for positive protein identification. This threshold was then used to compare syd immunoisolations and their respective negative controls. Proteins with a minimum of a 2-fold increase in spectra counts relative to their respective control were included in the final list (supplemental Data S1). Proteins with only one peptide identified were excluded.

Gene Ontology Analyses—We used a hypergeometric test in our Gene Ontology analysis. The reference group was represented by the sum of all the proteins identified in our mass spectrometry analysis. Each subgroup represented one immunoisolation: synaptic vesicles, small syd vesicles, or large syd vesicles. Proteins within each vesicle category were connected to biological process annotations provided by the Gene Ontology Consortium. Based on the hierarchical structure of the Gene Ontology annotations, the probability that each immediate daughter term (a *p* value) was linked to the number of selected genes by chance was calculated, as described in Ref. 30. We selected 25 representative Gene Ontology biological process terms, with at least one of the three categories having a *p* value inferior to 0.05, to construct the table shown in Fig. 4*B*. The full tables containing the 142, 67, and 86 Gene Ontology terms can be viewed in supplemental Data S2, S3, and S4 for the biological process, cellular component, and molecular function categories, respectively.

Sciatic Nerve Ligation—Sciatic nerve ligation experiments were performed as described previously (16). Briefly, the sciatic nerves of mice were ligated unilaterally at the midpoint, and mice were sacrificed at the indicated time after surgery. To avoid contamination of proximal and distal parts, two ligations were placed 1 mm apart. For biochemistry, equal lengths of the proximal and distal parts were homogenized in sample buffer, and equal protein amounts were loaded and analyzed by SDS-PAGE and Western blotting. The tubulin Western blot serves as loading control. For *in vivo* labeling of the endocytic pathway, two ligations were placed 1 mm apart, the nerve was sectioned in between the two knots, and 5 μl of 20 mg/ml Texas Red dextran 3000 MW (Molecular Probes) was injected in the rear leg footpad. All surgeries were performed using adult female C57/bl6 mice and anesthetized with isofluorane. All procedures were approved by the Washington University in St. Louis, School of Medicine, Animal Studies Committee.

Immunofluorescence—Sciatic nerves were dissected and postfixed 2 h in 4% paraformaldehyde in PBS. Nerves were incubated overnight in 20% sucrose, embedded in Tissue-Tek OCT medium, and frozen in dry ice-cooled methanol. Serial 10-μm cryostat sections were cut and mounted onto coated slides (Fisher Scientific). Sections were permeabilized and blocked with 10% goat serum, 0.1% Triton X-100 in PBS, or 5% fish skin gelatin, 0.3% Triton X-100 in PBS for 30 min. Sections were incubated with the indicated primary antibodies overnight at 4 °C and with Alexa Fluor-conjugated secondary antibodies for 3 h. For low resolution images, sections were observed with a ×20 objective on a Nikon TE2000. For high resolution images, sections were observed with a ×100 objective on an Olympus FV500 confocal microscope or a Nikon Optigrid and deconvolved using Metamorph software.

RESULTS

syd Is Associated with Vesicles of Distinct Size and Morphology—We previously reported that in peripheral nerves, syd is transported in both the anterograde and the retrograde directions and that in response to injury, syd preferentially interacts with dynactin, resulting in a net increase in retrograde transport (16). To identify new mechanisms and molecules that regulate the vesicular transport of signals in axons, we developed a purification strategy based on syd antibody conjugated to magnetic beads. As starting material, we used synaptosomes prepared from adult mouse cortex, which in addition to synaptic vesicles contain anterogradely transported vesicles as well as vesicles departing from the synaptic terminal toward the cell body. Synaptosomes thus allowed us to isolate syd-associated vesicles without a bias toward any specific transport direction. We first performed a subcellular fractionation of mouse cortices according to the procedures originally described by Huttner *et al.* (29, 31) (Fig. 1*A*). According to the original fractionation scheme, proteins enriched in synaptic and small vesicles are present in the LP2 fraction, whereas proteins present on larger vesicles and on presynaptic membranes are enriched in the LP1 fraction. Western blot analysis showed that, as expected, the synaptic vesicle markers synaptophysin and synaptobrevin/VAMP were enriched in the LP2 fraction, whereas the presynaptic protein SNAP25 was mainly found in the LP1 fraction (Fig. 1*B*). Importantly, a plasma membrane marker (Na^+/K^+ exchanger) and a mitochondrial marker (COX4) were de-enriched from the LP2 fraction (Fig. 1*B*), indicating that the LP2 fraction was not contaminated with large amounts of mitochondria or plasma membrane remnants. syd, kinesin heavy chain (KIF5C), the dynactin subunit anti-$p150^{Glued}$, and JNK3 were distributed throughout the gradient, *i.e.* they were present in the LP2 fraction but were not enriched relative to other fractions. The lack of enrichment of the molecular motors and JNK3 is consistent with these proteins being associated with various organelles. In addition, these proteins are peripheral membrane-associated and can thus be released from membrane compartments at every fractionation step. Furthermore, although the main site of function of synaptic vesicle proteins is the synapse, molecular motors and associated proteins are required from the cell body to the synapse.

The next purification step involved centrifugation of the LP2 fraction on sucrose velocity gradients and allowed us to separate vesicles according to their size (Fig. 1*A*). The synaptic vesicle markers synaptophysin and VAMP were highly enriched in fractions 3 and 4 (SVP) as expected (Fig. 1*C*). Electron microscopy (EM) analyses of fractions 3 and 4 confirmed the presence of mostly small size synaptic vesicles, together with vesicles of up to 100 nm in diameter (Fig. 1*D*). The presynaptic protein SNAP25 was mostly detected in fractions 8, 9, and 10 (LVP), which correspond to larger size organelles and presynaptic membranes (Fig. 1, *C* and *E*). syd, JNK, KIF5C, and anti-$p150^{Glued}$ were detected in both small and large size organelle fractions (Fig. 1*C*). The relatively high abundance of syd, JNK, and the molecular motors in fractions 1 and 2 corresponds to the non-membrane-associated pool. The presence of the Na^+/K^+ exchanger in fractions 8, 9, and 10 indicates the possibility of plasma membrane remnants or its association with large vesicles for transport to the presynaptic membrane.

Immunoisolation of syd-associated Vesicles—To identify syd-associated vesicles, we next used a purification strategy based on anti-syd antibodies conjugated to Dynabeads. syd antibodies or preimmune serum (as a negative control) were linked to anti-rabbit-coated Dynabeads. syd vesicles were immunoisolated from both the SVP and the LVP fractions. To evaluate the specificity of the immunoisolation procedure and provide an internal control, we used anti-synaptotagmin antibodies linked to Dynabeads to immunoisolate synaptic vesicles from the SVP. Electron microscopy of negative control beads revealed a smooth bead surface with no vesicles or membranes attached (Fig. 2, *A* and *D*). The anti-synaptotagmin-coated Dynabeads were decorated with small vesicles of diameter of 30–50 nm, which is in agreement with the previously reported morphological characteristics of synaptic vesicles (Fig. 2*B*) (3–7). In marked contrast, the anti-syd-coated beads showed a more heterogeneous distribution of vesicle size and morphology (Fig. 2*C*). Overall the diameter ranged from 100 to 200 nm with occasional tubule-like morphology. Our EM analyses thus revealed that two different types of vesicles were isolated from the same starting material and that small syd vesicles are morphologically distinct from synaptic vesicles. We next examined syd vesicles isolated from the LVP and observed an endosomal/multivesicular morphology (Fig. 2*E*).

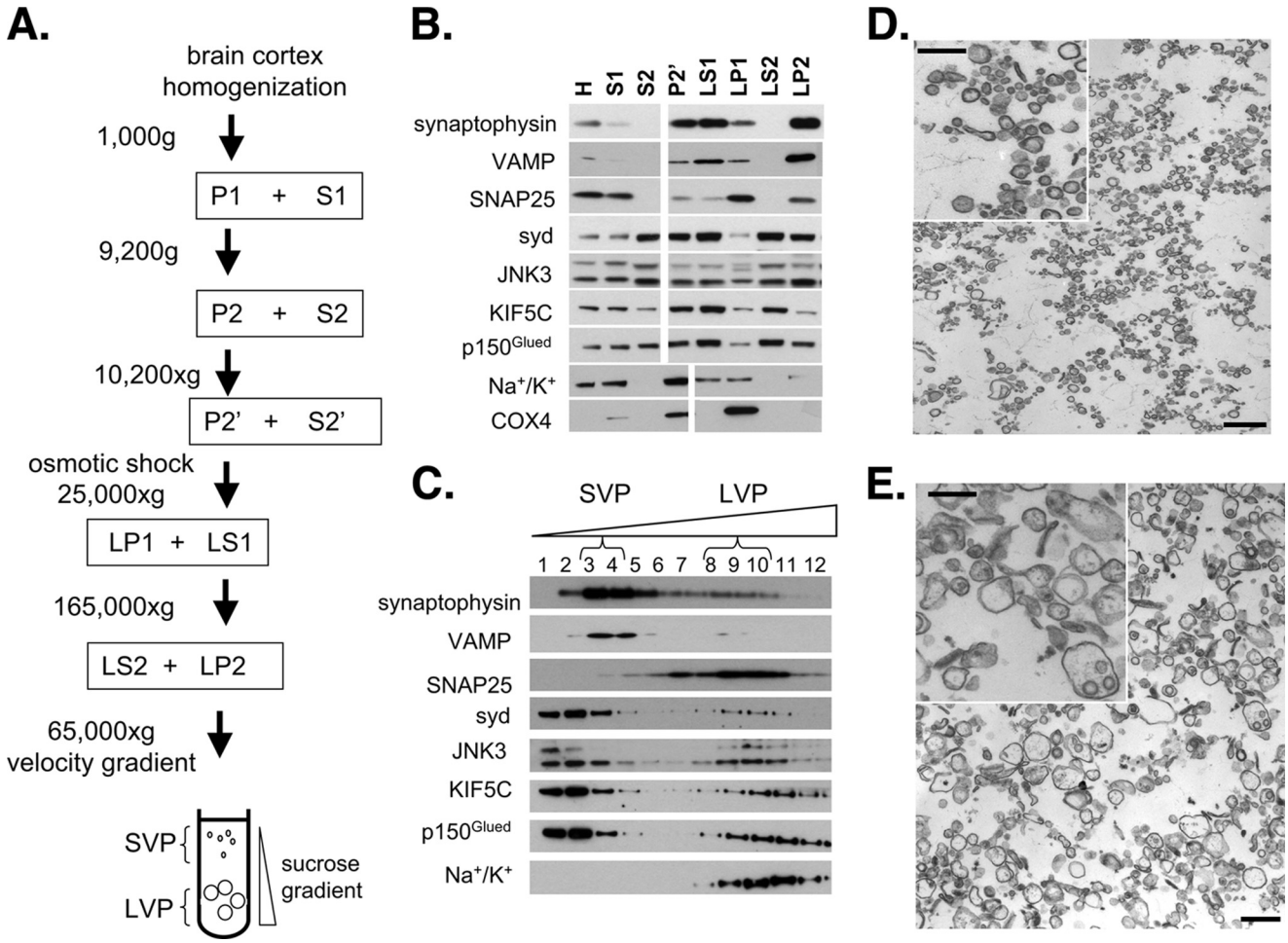

FIGURE 1. **syd and the molecular motors are associated with vesicles of distinct size.** *A*, schematic diagram of the synaptosome preparation method, modified from Ref. 29. *B*, mouse brain cortex was fractionated by differential centrifugation to obtain a synaptosome-enriched fraction LP2. syd, JNK, and the molecular motors are present in the LP2 fraction, which is enriched with the synaptic vesicle markers synaptophysin and VAMP. The lack of enrichment of these proteins in the LP2 fraction is consistent with these proteins being associated with various organelles and the presence of large soluble populations. *C*, following sedimentation of the LP2 fraction on a sucrose velocity gradient, two distinct vesicles pools were obtained. Small vesicles containing synaptic vesicle markers were detected in fractions 3 and 4 (SVP). Larger vesicles containing the presynaptic membrane protein SNAP25 were detected in fractions 8, 9, and 10 (LVP). syd, JNK, and the molecular motor proteins were detected in both small and large vesicles fractions. *D*, electron microscopic analysis of pooled fractions 3 and 4 revealed the presence of synaptic vesicles of 30–50 nm in diameter together with other organelles of up to 100 nm in diameter. *E*, EM analysis of pooled fractions 8, 9, and 10 revealed a more heterogeneous profile of organelles, vesicles, and tubules ranging from 100 to 500 nm. In *D* and *E*, *bar* = 400 nm; in the *inset*, *bar* = 200 nm.

To confirm the endosomal nature of syd vesicles in the LVP, we immunoisolated endosomes using antibodies against Rab5, a marker for endosomes, and observed predominantly multivesicular organelles (Fig. 2*F*), similarly to syd vesicles and to what has been previously described (32, 33). Together, these results suggest that syd is associated with at least two classes of vesicles. Small syd vesicles are distinct from synaptic vesicles, and large syd vesicles display an endosomal morphology. This is in agreement with our previous electron microscopy studies of syd vesicles in peripheral nerves in which we showed that syd associates with both small vesicles and larger, multivesicular organelles (16).

We then analyzed the immunoisolated material by SDS-PAGE and Western blot. As expected, the classical synaptic vesicle markers synaptophysin and VAMP were isolated on anti-synaptotagmin-coated beads from the SVP fraction (Fig. 3*A*). In contrast, these purified vesicles did not contain significant amounts of syd. Likewise, purified syd vesicles from the same SVP fraction did not contain significant amounts of synaptophysin, synaptotagmin, or VAMP (Fig. 3*A*). Western blot analyses of syd vesicles immunoisolated from the LVP fraction revealed the presence of the early/recycling endosomal proteins VAMP3/cellubrevin, syntaxin 13, and clathrin (Fig. 3*B*). In contrast to syd vesicles immunoisolated from the SVP, syd vesicles immunoisolated from the LVP contained synaptophysin and syntaxin 1, suggesting that syd may function to transport synaptic vesicle components to the synapse or may participate in the recycling of synaptic vesicle components after synaptic vesicle fusion. Western blot analyses also revealed the presence of the kinesin heavy chain KIF5C and of the dynactin subunit anti-p150^{Glued} (Fig. 3*B*) but lower amounts of the KIF3A subunit of heterotrimeric kinesin-2. This result is in agreement with previous observations that KIF3A/B-associated vesicles purified from mouse brain are distinct from endosomal/multivesicular syd vesicles, displaying a relatively uniform morphology with a diameter of 90–160 nm (34).

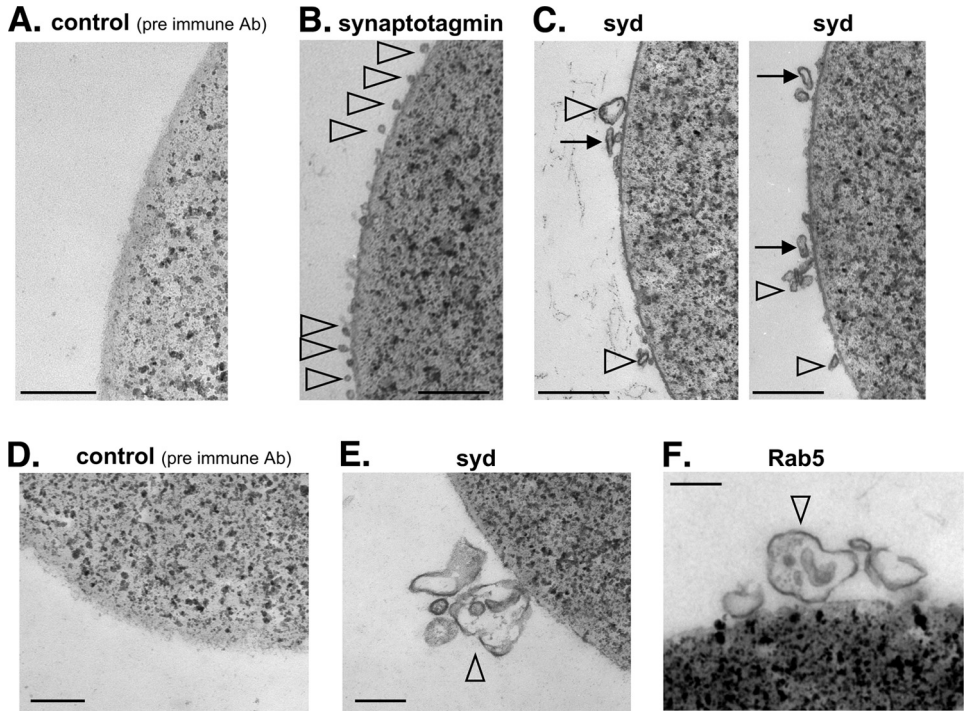

FIGURE 2. **Electron microscopic analysis of immunoisolated syd vesicles.** SVP (*A–C*) or LVP (*D–F*) were incubated with magnetic beads coated with the indicated antibody (*Ab*). *A*, control beads coated with preimmune serum were devoid of any membrane profiles. *B*, vesicles from fractions 3 and 4 adsorbed to the anti-synaptotagmin beads revealed the expected profile for 30–50-nm synaptic vesicles. *C*, membranes from fractions 3 and 4 adsorbed to anti-syd beads were composed of 100–200 nm small single membrane vesicle (*arrowheads*) and tubules (*arrows*). *D*, control beads coated with preimmune serum and incubated with the LVP were devoid of any membrane profiles. *E*, membranes adsorbed to anti-syd beads from the LVP were composed primarily of large, multivesicular vesicles of up to 500 nm. These membrane profiles are similar to endosomes adsorbed on anti-Rab5 beads. In *A–F*, *bar* = 200 nm.

Although the amount of plasma membrane contamination in SVP was relatively low (Fig. 1*B*), plasma membrane proteins may have co-purified with the LVP, as shown by the distribution of the plasma membrane marker Na^+/K^+ exchanger in the sucrose velocity gradient (Fig. 1*B*). However, we can exclude the possibility that plasma membrane was a major contaminant in our syd vesicle isolation because only traces of the Na^+/K^+ transporter were detected by Western blot in syd vesicles immunoisolated from the LVP (Fig. 3*B*). In addition, the Na^+/K^+ exchanger is also endocytosed, and its presence in the Rab5 and Rab11 isolation may reflect its association with endosomes (Fig. 3*D*). Together, our electron microscopy and biochemical analyses suggest that syd associates with at least two distinct types of vesicles. One class of small vesicles is distinct from classical synaptic vesicles and another class of larger vesicles may represent a population of endosomes.

Identification of the Protein Composition of syd Vesicles by Mass Spectrometry—To gain further insights into the nature of syd-associated vesicles, we next determined the protein composition of synaptic and syd-associated vesicles by mass spectrometry analysis (nano-LC-MS/MS). The protein composition of each vesicle class as well as their respective negative control was determined (see "Experimental Procedures"). We used spectra count as a semiquantitative measure of protein abundance in each category. The enrichment of each protein is thus a relative measure of abundance and not an absolute value. Only proteins with a minimum of a 2-fold increase in spectra count relative to their respective control were included in the final list (supplemental Data S1 and see Experimental Procedures). In total, 111, 169, and 352 proteins were identified in synaptic vesicles, small syd vesicles, and large syd vesicles, respectively. Each vesicle population contained common and unique proteins (Fig. 4*A* and see supplemental Data S1). Gene Ontology analysis indicated that, similarly to our biochemical and EM analyses, small and large syd vesicles are distinct from each other, and both are distinct from synaptic vesicles (Fig. 4*B* and see "Experimental Procedures"). Proteins within each vesicle category were connected to biological process annotations provided by the Gene Ontology Consortium, and the probability that each immediate daughter be linked to the number of selected genes by chance was calculated. Out of 142 Gene Ontology terms in the biological process category with at least one of the three categories having a *p* value inferior to 0.05, we selected 25 representative Gene Ontology terms to build the illustrated table (Fig. 4*B*). The complete tables for the biological process, cellular component, and molecular function categories are available as supplemental Data S2, S3, and S4, respectively. To further characterize small and large syd vesicles, we grouped the 39 and 194 proteins unique to small and large syd vesicles, respectively, in functional categories (Fig. 4*C*). This analysis revealed that small and large syd vesicles are functionally distinct. Fewer RNA processing- and signaling-related proteins and more trafficking and endocytosis and synaptic-related proteins were found in large syd vesicles. The tables containing the full complement of proteins grouped according to their known or putative function are shown in supplemental Data S4 and S5.

Synaptic Vesicles—Out of 111 identified proteins in our anti-synaptotagmin immunoisolation, most are previously defined components of synaptic vesicles (supplemental Data S1) and were also positively identified by Takamori *et al.* (3). These include small GTPases (Rab2, Rab3, Rab5, and Rab11), endocytosis-related proteins (clathrin adaptor proteins), motor proteins (dynein light chain), cytoskeleton (Arp2/3), trafficking proteins (syntaxin 12, synaptotagmin, synaptobrevin/VAMP), transporter and channels (vacuolar ATPase, Na^+/K^+ exchanger), and metabolic enzymes (glutamate decarboxylase, creatine kinase). The smaller number of identified proteins in our analysis when compared with the results of Takamori *et al.* (3) may reflect the different techniques employed to obtain purified synaptic vesicles. In addition to the subcellular fractionation to obtain a homogenous population of small vesicles,

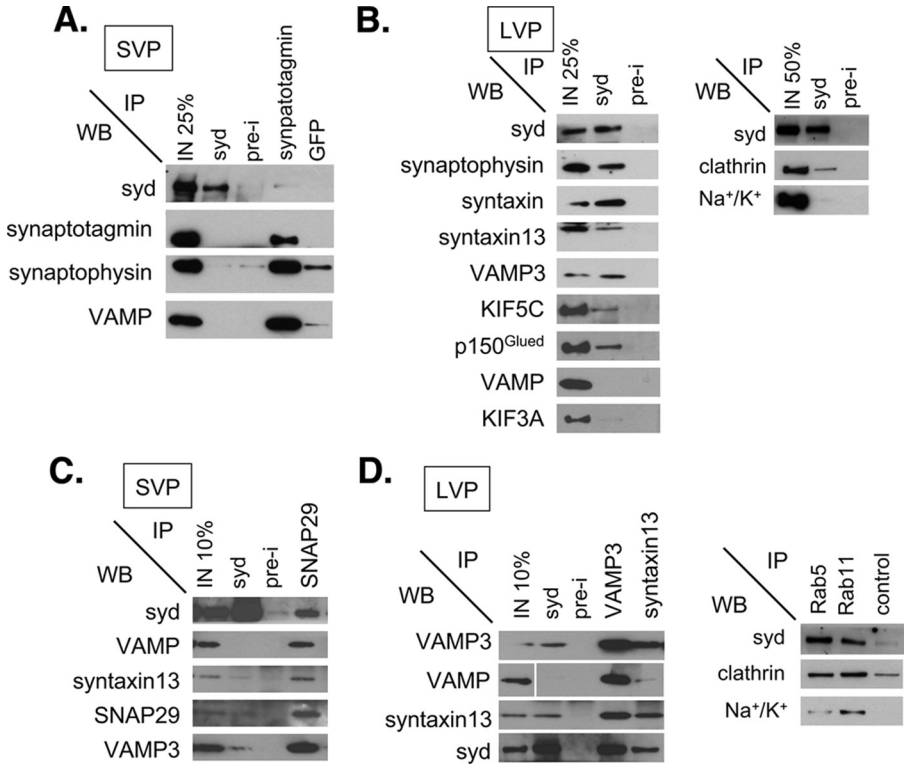

FIGURE 3. **Western blot analysis of immunoisolated syd vesicles.** Vesicles immunoisolated from SVP (*A* and *C*) or LVP (*B* and *D*) using the indicated antibodies were analyzed by Western blot (*WB*). Efficiency of isolation was estimated at ~20% for both SVP and LVP fractions. *A*, small syd vesicles were distinct from synaptic vesicles. Immunoisolation with syd antibodies did not contain components of synaptic vesicles such as synaptotagmin, synaptophysin, or VAMP, and reversely, immunoisolated synaptic vesicles on anti-synaptotagmin-coated beads did not contain syd. *IP*, immunoprecipitation; *pre-i*, preimmune serum used as a negative control; *IN*, percentage of input material for the immunoisolation; *GFP*, green fluorescent protein. *B*, large syd vesicles contained the endosomal markers syntaxin 13, VAMP3, and clathrin, but no detectable VAMP or Na^+/K^+ exchanger. The motor proteins KIF5C and anti-$p150^{Glued}$ were detected in large syd vesicles, but no significant amount of the other kinesin motor KIF3A was detected, in agreement with syd being an adaptor for the conventional kinesin-1 motor. *C* and *D*, reverse immunoisolations were performed using antibodies against proteins identified by mass spectrometry. *C*, beads coated with anti-SNAP29 isolated vesicles containing syd. *D*, immunoisolation using the indicated endosomal markers isolated syd, indicating that syd in part resides on endosomes. The input material is 10% for all immunoisolations, except for VAMP, which is 20%.

we performed immunoisolation on anti-synaptotagmin-coated magnetic beads to reduce contamination by small trafficking vesicles of different origin. This result thus supports the validity of our approach to immunoisolate distinct vesicle populations.

Small syd Vesicles—Small syd vesicles and synaptic vesicles were both purified from the SVP. Only 29 proteins co-purified with both synaptic vesicles and small syd vesicles, and 23 of these proteins were common to all three vesicles categories (Fig. 4*A* and supplemental Data S1). Proteins common to small syd vesicles and synaptic vesicles included the vacuolar ATPase, the small GTPase Rab5, clathrin coat assembly AP50, and synaptoporin. Proteins present exclusively in small syd vesicles included trafficking-related proteins (synaptotagmin VII, SNAP29), signaling proteins (sprouty, Minkk1 kinase, casein kinase), cell adhesion proteins (neogenin, neurocan), cytoskeletal proteins, and ribosomal proteins. To validate our results, we then performed reverse immunoisolation experiments using antibodies against proteins identified on small syd vesicles. We selected the synaptosomal-associated protein SNAP29, which is involved in multiple membrane trafficking steps and localizes to intracellular membrane structures rather than to the plasma membrane. Anti-SNAP29-coated magnetic beads (Fig. 3*C*) revealed the presence of syd, VAMP, VAMP3/cellubrevin, and syntaxin 13. Immunoisolated syd vesicles contained low levels of SNAP29, syntaxin 13, and VAMP3/cellubrevin but not VAMP (Fig. 3*C*). The presence of VAMP on SNAP29 vesicles is in agreement with its role in regulating synaptic vesicle fusion (35). However, our data suggest that SNAP29 also resides on small syd vesicles, which are distinct from synaptic vesicles. The promiscuous interaction of SNAP29 with several syntaxins may contribute to altering the cycling efficiency of small syd vesicles and synaptic vesicles after fusion.

Large syd Vesicles—A larger number of proteins were identified in large syd vesicles, reflecting the greater detection limit due to increased amounts of material employed for the immunoisolation. A large proportion of proteins identified was unique to large syd vesicles, with some overlap with small syd vesicles and synaptic vesicles (Fig. 4*A* and supplemental Data S1). Among the proteins identified were molecular motors (dynein, kinesin heavy chain, Myosin Va), trafficking-related proteins (Rab15, Rab18, RabGDI), endosomal proteins (Rab5, Rab7, Rab11, dynamin, AP180, neurobeachin, AP2, amphiphysin, clathrin), ubiquitin-related proteins (ubiquitin carboxyl-terminal hydrolase 5, Phr1, Cullin-associated NEDD8-dissociated protein 1), signaling proteins (adenylate cyclase, phosphoinositide kinases), and transporter and channels and cytoskeletal proteins. The protein composition (Fig. 4*C* and supplemental Data S1) combined with the vesicle morphology analyses by EM (Fig. 2, *E* and *F*) suggest that large syd vesicles belong to the endocytic pathway. To further test the endocytic nature of large syd vesicles, we performed immunoisolation from the LVP using identified endosomal markers. The small GTPase Rab5 and Rab11, syntaxin 13, and VAMP3/cellubrevin are well characterized markers of early/recycling endosomes (36, 37). Beads coated with anti-VAMP3/cellubrevin or anti-syntaxin 13 isolated syd, VAMP3/cellubrevin, and syntaxin 13, and syd isolated both VAMP3 and syntaxin 13 (Fig. 3*D*, *left panel*). Synaptobrevin/VAMP was detected mainly in the VAMP3/cellubrevin immunoisolation, with only traces in the syntaxin 13 immunoisolation. VAMP3/cellubrevin vesicles may represent synaptic vesicle precursors, in agreement with the localization of VAMP3/cellubrevin on classical synaptic vesicles containing VAMP (3) and the presence of both

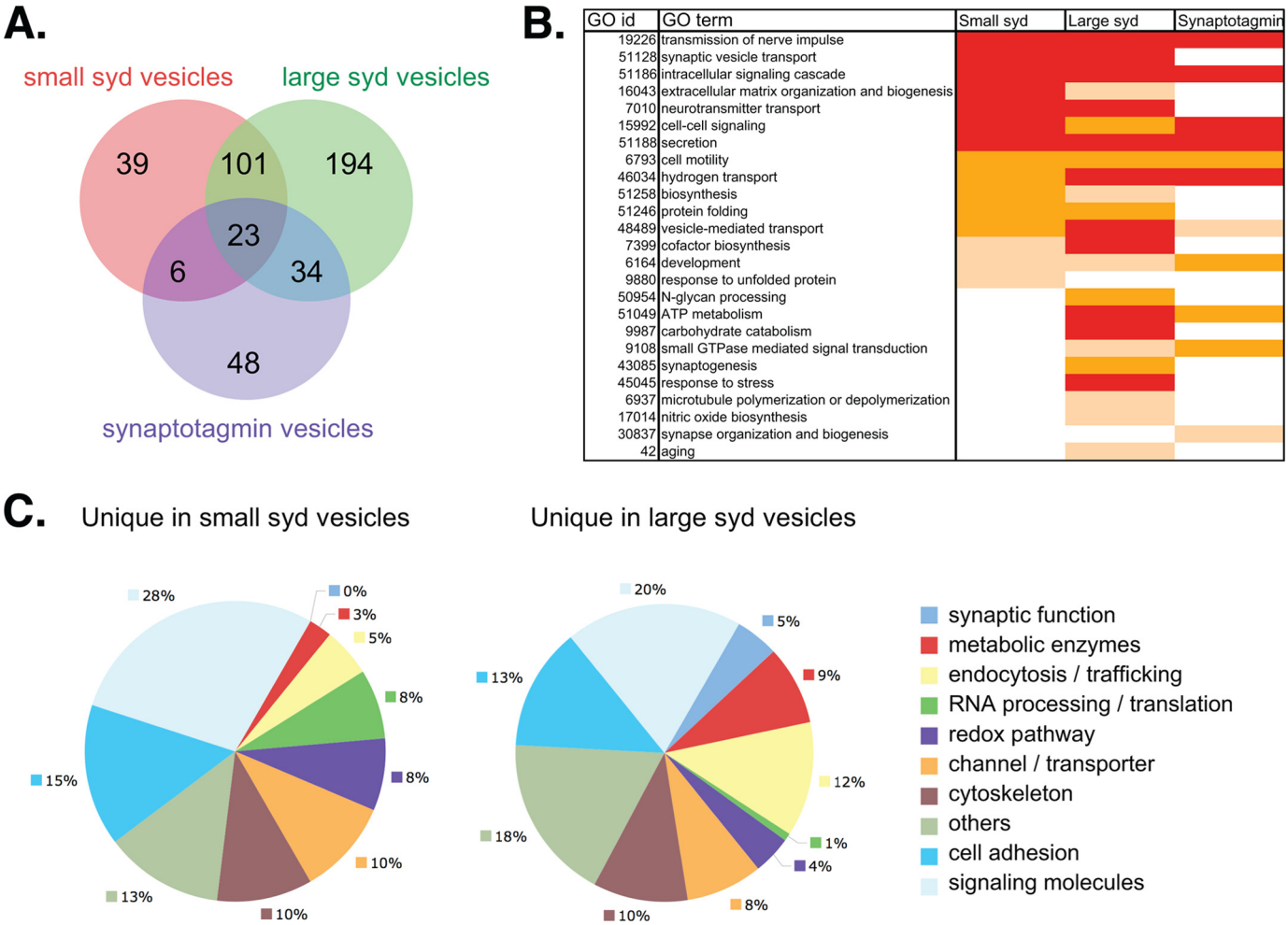

FIGURE 4. **Mass spectrometry and Gene Ontology analysis.** *A*, the protein composition of synaptic and syd-associated vesicles was determined by mass spectrometry analysis. Spectra counting, *i.e.* the number of peaks detected for a particular protein, was used as a relative quantification between each sample and their negative control. The synaptic vesicle protein composition provided a positive control to determine the minimal -fold difference in spectra counts between syd immunoisolations and their respective negative controls. Thus, only proteins with a minimum of a 2-fold higher value in spectra count relative to their respective control were included in the final list (supplemental Data S1). A Venn diagram was created to indicate the protein composition overlap between the three types of vesicles. *B*, proteins within each vesicle category were connected to biological process annotations provided by the Gene Ontology (*GO*) Consortium. Based on the hierarchical structure of the Gene Ontology annotations, the probability that each immediate daughter term (a *p* value) be linked to the number of selected genes by chance was calculated. This analysis revealed that small and large syd vesicles are distinct from each other and that both are distinct from synaptic vesicles. Out of 142 GO terms in the biological process category with at least one of the three categories having a *p* value inferior to 0.05, we selected 25 representative GO terms to build the illustrated table. The complete tables are available as supplemental Data S2, S3, and S4 for the biological process, cellular component, and molecular function categories, respectively. *Red*, *p* value ≤0.001; *orange*, *p* value >0.001 and ≤0.01; *light orange*, *p* value >0.01 and ≤0.05; *white*, *p* value >0.05. *C*, the 39 and 194 proteins unique to small and large syd vesicles, respectively, were grouped in functional categories. Fewer RNA processing- and signaling-related proteins and more trafficking and endocytosis and synaptic-related proteins were found in large syd vesicles.

proteins on same vesicles (37). The variation in the immunoisolation efficiency for each of the three proteins indicates that these proteins do not have identical subcellular distributions but co-localize partially in endocytic organelles. Using anti-Rab5- or anti-Rab11-coated magnetic beads, syd and the endosomal protein clathrin were immunoisolated (Fig. 3*D*, *right panel*). Low levels of the Na^+/K^+ exchanger protein were detected in the Rab5 immunoisolation, consistent with a role of Rab5 in the transport of plasma membrane-derived clathrin-coated pits toward early endosomes. The negative controls indicate that there was a very small amount of background binding of either organelles or protein complexes to the magnetic beads (Fig. 3), which might explain the presence of ribosomal and mitochondrial proteins detected on large syd vesicles (supplemental Data S1). In contrast to the SVP fraction, the LVP fraction may be contaminated with small amounts of postsynaptic, dendritic, or soma-derived organelles and protein complexes. A small proportion of isolated syd vesicles may thus reflect syd association with non-axonal compartments and mitochondria (38, 39). Nonetheless, large syd vesicles may represent at least in part a population of early/recycling endosomes. Recent observations that the highly related and ubiquitous protein JIP4/JLP is associated with Rab5-containing early endosomes in Hela cells (40) and mediates endosomes to trans-Golgi network transport (41) further support these conclusions.

In Vivo Validation of Components of syd Vesicles—Our biochemical analyses revealed the isolation of two populations of syd vesicles with distinct protein composition and morphology.

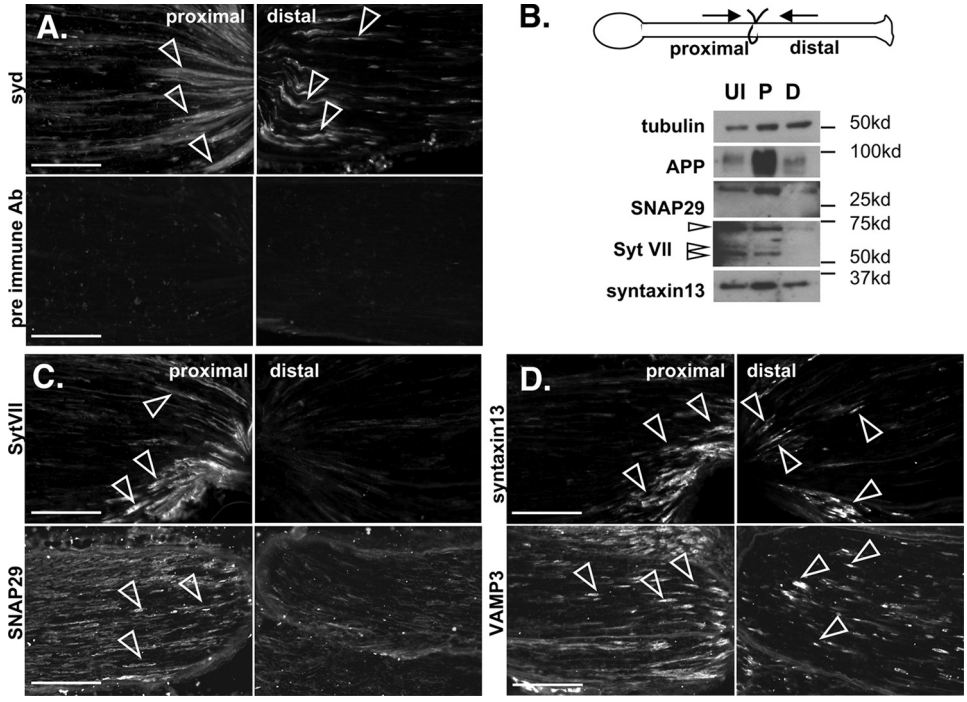

FIGURE 5. **Axonal transport of syd vesicle components.** Sciatic nerves were ligated unilaterally at the midpoint and processed for immunofluorescence microscopy or SDS-PAGE and Western blot analysis. *A*, syd accumulates on both the proximal and the distal side of the ligation site, as expected. *Ab*, antibody. *B*, ligated and contralateral unligated sciatic nerves were dissected. and extracts were analyzed by Western blot with the indicated antibodies. SNAP29 and synaptotagmin VII (*SytVII*), two proteins identified on the small syd vesicles, accumulated mostly on the proximal side, indicative of anterograde transport. Low levels are also detected to some extent on the distal sides, similarly to amyloid precursor protein (*APP*), a well established anterograde marker. The synaptotagmin antibody recognizes several isoforms, as indicated. Syntaxin 13, identified on the large syd vesicles, was detected on both the proximal and the distal sides, indicating that these proteins are transported in both anterograde and retrograde directions. Tubulin is used as a loading control. *UI*, unligated; *P*, proximal; *D*, distal. *C* and *D*, SNAP29 and synaptotagmin VII are found mostly on the proximal side (*C*), and syntaxin 13 and VAMP3 are found on both sides (*D*), similarly to syd. In *A*, *C*, and *D*, *bar* = 100 μm.

Our previous immuno-EM analyses showed that in mouse sciatic nerve, anterogradely moving syd-associated vesicles are mostly small vesicles/tubules and retrogradely transported syd vesicles are larger, often multivesicular organelles (16). Small syd vesicles may belong to the anterograde pathway, whereas large syd vesicles may belong mainly to the retrograde pathway. To test this possibility, we used sciatic nerve ligation experiments, which allowed us to assess *in vivo* the transport properties of several markers identified in each syd vesicle category. Mouse sciatic nerves were subjected to ligations, and nerve portions proximal or distal to the ligation site were analyzed by immunofluorescence microscopy and Western blotting. Proteins moving in the fast anterograde axonal transport pathway generally accumulate on the proximal side of a ligation, whereas proteins moving in the anterograde and retrograde pathways generally accumulate on both proximal and distal sides. Slow moving or non-axonal proteins remain unchanged. Immunofluorescence of longitudinal sections of a ligated nerve revealed accumulation of syd on both sides of the ligature (Fig. 5*A*), as reported previously (16). Proteins identified in the small syd vesicle population, SNAP29 and SytVII, accumulated mostly proximal to the ligation site, indicative of anterograde axonal transport, as predicted (Fig. 5, *A* and *B*). In contrast, proteins identified on the large syd vesicle population, such as VAMP3/cellubrevin and syntaxin 13, accumulated on both proximal and distal sides, indicative of bidirectional transport (Fig. 5, *B* and *D*). Our results indicate that morphologically and biochemically distinct syd vesicles display distinct axonal transport properties. Small syd vesicles primarily travel in the anterograde direction, and syd-endosomes may travel bidirectionally, consistent with the presence of both kinesin and dynein-dynactin and with previous observations that early/recycling endosomes travel bidirectionally along axons of culture neurons (42, 43). Alternatively, syd may function as a motor adaptor to transport small vesicles in the anterograde pathway and then switch to transport endosomes in the retrograde direction. Together, these findings suggest that syd may thus play different roles in axonal growth, maintenance, or repair.

In Vivo Co-localization of syd with Endosomes—Our previous immuno-EM analyses in sciatic nerve indicated that syd localizes to multivesicular organelles on the distal side of a ligation (16), but these experiments did not demonstrate whether these organelles belong to the endocytic pathway. To address whether syd plays a role in endosomal trafficking along axons *in vivo*, we labeled the endocytic pathway in peripheral nerves and examined syd co-localization with labeled endosomes by fluorescence microscopy. We labeled the endocytic pathway in sensory neurons by subcutaneous injection of the endocytic tracer Texas Red dextran in the mouse rear leg footpad. Nerves are able to take up tracers at the sensory terminals and transport them retrogradely along axonal tracts to the cell body in the dorsal root ganglia. We performed a sciatic nerve ligation concomitant with dye injection to increase the number of labeled structures accumulating distal to the ligation site. The sciatic nerve was analyzed 24 h after injection. Distal to the ligation site, axons labeled with Texas Red dextran contained syd (Fig. 6*A*). In contrast, proximal to the ligation site, no dextran was detected, but syd accumulated, as expected (Figs. 5*A* and 6*A*) (16). When examined at higher magnification (Fig. 6*B*) or by confocal microscopy (Fig. 6*C*) followed by deconvolution, Texas Red dextran-positive structures partially co-localized with syd within single axons. Structures positive for syd and Texas Red dextran also partially co-localized with the endosomal marker VAMP3 (44) (Fig. 6*D*), which we found associated to large syd vesicles (Fig. 3*D*). These results indicate that syd resides at least in part on axonal endosomes. However, the exact nature of the labeled endosomes awaits further investigation at the EM level. Together, our findings further our previous observations and show that syd asso-

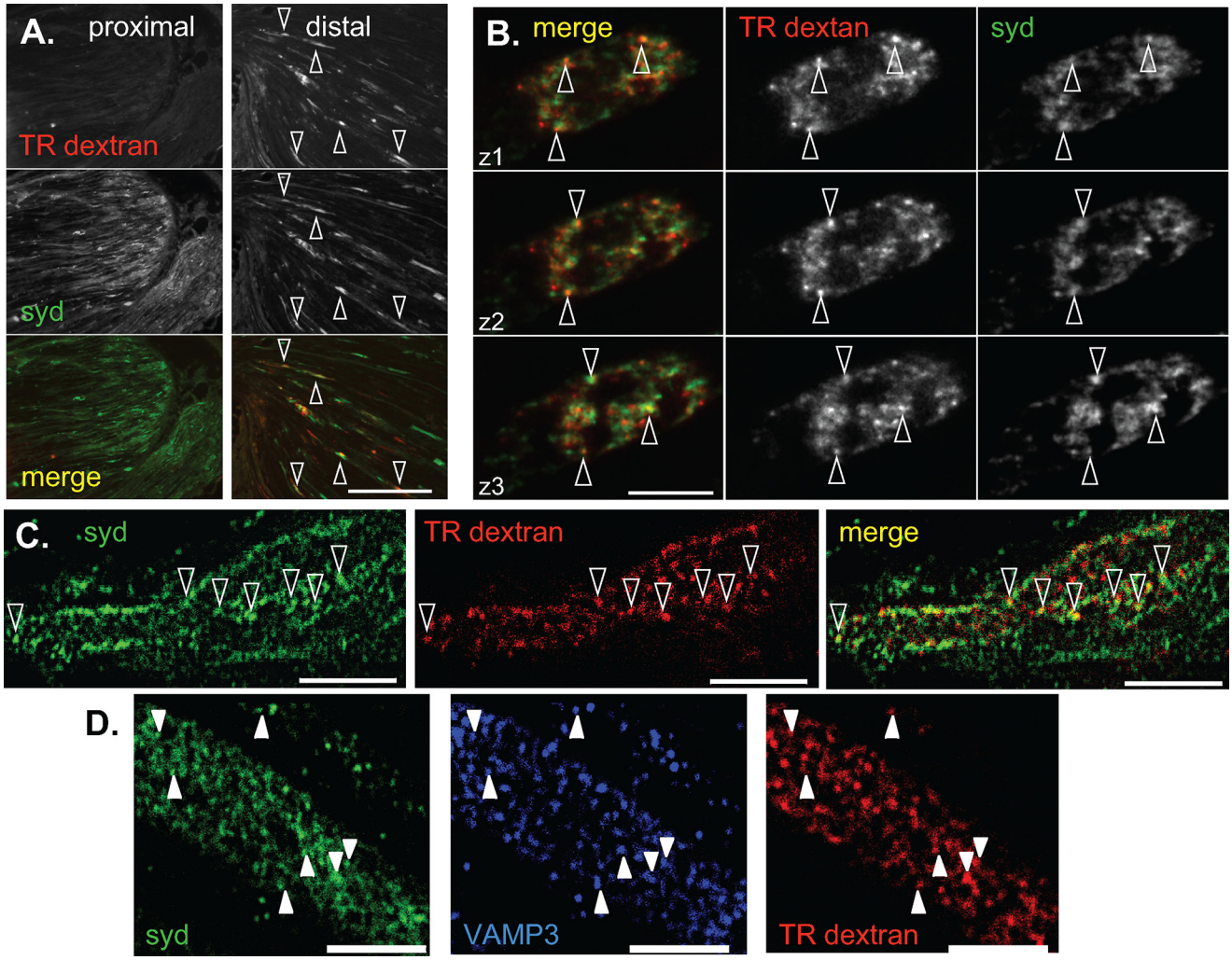

FIGURE 6. **syd localization with *in vivo* labeled endosomes.** The endocytic pathway within sensory neurons was labeled by subcutaneous injection of the tracer Texas Red dextran in the mouse rear leg footpad. A sciatic nerve ligation concomitant with dye injection was performed to increase the number of labeled structures accumulating distal to the ligation site. The sciatic nerve was dissected 24 h after injection, fixed, and embedded in cryomold. Longitudinal sections were analyzed by immunofluorescence. *A*, low magnification images showed syd accumulation in Texas Red dextran (*TR dextran*)-positive axons (*arrowheads*). *B* and *C*, Nikon Optigrid structured illumination microscopy (*B*) or confocal microscopy (*C*) followed by deconvolution showed that Texas Red dextran puncta partially co-localize with syd. Three consecutive sections in the *z* plane are shown in *B*. *D*, triple labeling immunostaining showed that syd-dextran-positive structures also contained the endosomal protein VAMP3/cellubrevin, further supporting the notion that syd resides at least in part on axonal endosomes. In *A*, *bar* = 100 μm; in *B–D*, *bar* = 5 μm.

ciates with two distinct axonal vesicle populations, thereby shedding light on the function of syd in both development and regeneration.

DISCUSSION

syd was previously characterized as a scaffolding protein, linking vesicular transport to injury signaling along axons (13–16). In this study, we have uncovered the molecular anatomy of syd-associated vesicles. We present the characterization of two distinct classes of syd-associated vesicles purified from synaptosomes using an immunoisolation approach. Synaptosomes are derived from adult mouse cortex and contain, in addition to synaptic vesicles, anterogradely transported vesicles, as well as vesicles departing from the synaptic terminal toward the cell body. Synaptosomes thus allowed us to isolate syd-associated vesicles without a bias toward any specific transport direction. Our analyses point to a role for syd in the transport of endosomes along the axons and at the synapse. Endosomes in neurons serve many purposes, including long range retrograde signaling (45), synaptic function (46), and synaptic plasticity (47). In addition, endosomal dysfunction may underlie the development of many neurodegenerative diseases (48). We suggest that syd-associated early/recycling endosomes function in part to carry injury signals from the injury site back to the cell body and may also regulate synaptic vesicle recycling. In addition, our data suggest that syd may play a role in axonal growth and guidance through its interaction with another class of small anterograde vesicles, although future studies will be required to test this prediction.

Role of syd in Endosomal Transport along the Axon—Our data suggest that syd vesicles represent a population of bidirectional early/recycling endosomes that utilize kinesin-1 and dynein-dynactin for transport along the axon (Figs. 3, 5, and 6). Movement of endosomes in axons was thought to be exclusively retrograde (49), but other studies have shown bidirectional movement of recycling endosomes (42) and late endo-

somes/lysosomes (50). More recently, live imaging experiments in cultured neurons revealed that the anterograde transport of endosomes mediates targeting of the adhesion molecule L1/Cam to the axon (43). We found L1/Cam in large syd vesicles (supplemental Data S1), suggesting that a syd-dependent recruitment of kinesin to endosomes may mediate L1/Cam transport to the axon. syd may represent a regulatory switch for motor proteins of opposing direction that controls trafficking of endocytic vesicles along the axon because the binding sites for kinesin and dynactin overlap (40).

Our *in vivo* labeling experiments in peripheral nerves (Fig. 6) indicate that syd partially localizes with endosomes that originated at the nerve terminal and are transported retrogradely to the nerve ligation site. Although proteins involved in signal transduction were identified in both small and large syd vesicles (Fig. 4*C*), we failed to detect the expected injury-signaling proteins such as JNK or the upstream kinases. As these proteins are peripheral membrane-associated, it is possible that they were released from membrane compartments during the final purification procedure. Alternatively, JNK and the related upstream kinases may be specifically associated with peripheral syd vesicles, as we previously showed (16), and not with synaptosome-derived syd endosomes. Future studies will determine the precise composition of syd-endosomes in peripheral nerves.

Once at the ligation site, syd-endosomes may contribute to local membrane trafficking events including exo- and endocytosis. Indeed, several studies have shown that exo- and endocytosis are required for plasma membrane repair in epithelial cells (51, 52). Although the endocytic pathway in epithelial cells is well characterized, the molecular machinery mediating endosomal trafficking in neurons is still poorly understood. Nonetheless, the emerging picture of endosomal trafficking in neurons suggests that different endosomal pools may be involved in the regulation of distinct signaling pathways and polarized distribution of guidance and adhesion molecules (2).

The retrograde transport of endosome/multivesicular bodies (MVBs) is believed to represent the organelle that carries neurotrophic factors in axons. Although the brain-derived neurotrophic factor TrkB receptor was identified on syd vesicles (supplemental Data S1), our data do not allow us to establish whether syd mediates the retrograde transport of the classical neurotrophin-signaling endosome. Furthermore, the role of MVBs in retrograde signaling endosomes in axons has been recently challenged (53), and MVBs may instead represent a population of organelles that arises upon injury in axons. Indeed, MVBs retrograde transport may play a role in injury signaling. Storage of signaling molecules within intralumenal vesicles of multivesicular bodies may prevent their deactivation during the long journey from the axon back to the cell body (54). Kinases such as JNK can hitchhike on axonal vesicles (16), and intralumenal vesicles are not always destined for lysosomal degradation; they can also fuse back with the limiting membrane of late endosomes (55). This process is hijacked by several toxins and viruses to reach the cell body and could similarly be exploited by signaling proteins (55). For example, storage of phosphorylated proteins within intralumenal vesicles may allow effective long range signaling in neurons and may play an important role in nerve regeneration.

syd Function in Synaptic Vesicle Recycling—In addition to a role in regulating endosomal trafficking along the axon, syd may play a role in Rab5-dependent endosomal trafficking processes at the synapse. Our observations that syd associates with Rab5-containing endosomes (Fig. 3) is in agreement with the recent finding that loss of function of *unc-16*, the *Caenorhabditis elegans* homolog of syd, leads to an accumulation of enlarged Rab5-containing compartments and a decrease in the number of synaptic vesicles in GABAergic synapses (56). syd may thus participate in the recycling of synaptic vesicle components after synaptic vesicle fusion. Because syd endosomes contain the synaptic vesicle proteins synaptophysin and syntaxin 1, syd may also function to transport synaptic vesicle components to the synapse, similarly to its *C. elegans* homolog *unc-16*. Indeed, loss of function of *unc-16* also results in mislocalization of synaptic vesicle marker synaptobrevin (57, 58). In addition, UNC-16 interacts with UNC-14 (58), which is involved in the regulation of synaptic vesicle localization and functions in the same pathway as *unc-16*. syd may thus play a key role in synaptic transmission by regulating synaptic vesicle formation and recycling.

Possible Roles for syd in Axonal Growth—The precise nature and function of the small syd vesicles await further studies. However, the presence of adhesion and cytoskeletal regulatory proteins as well as ribosomal proteins (Fig. 4), together with the observation that small syd vesicles mainly travel in the anterograde pathway (16) (Fig. 5), lead us to propose that small syd vesicles may play a role in neurite outgrowth and guidance. This hypothesis is supported by the axonal growth defects observed in syd knock-out animals (17, 18). Another link between syd and axonal growth and guidance comes from *C. elegans* studies. In addition to its interaction with syd/UNC-16, UNC-14 is a direct regulator of the protein kinase UNC-51, and both are required for axonal elongation and guidance (59). If small syd vesicles play a role in axonal outgrowth during development, they may serve a similar role during nerve repair and regeneration. Synaptotagmin VII, a member of the synaptotagmin family of Ca^{2+}-binding proteins, was identified in small syd vesicles. Synaptotagmin VII mediates exocytosis of lysosomes, a process important for the repair of plasma membrane wounds (52) and for neurite outgrowth (27).

In summary, we have uncovered the molecular anatomy of two distinct classes of syd-associated vesicles. Our studies point to a role for endocytic syd vesicles in the transport of signals along the axon and in the recycling of synaptic vesicles. In addition, syd may play a role in axonal growth and guidance through its interaction with another class of small anterograde vesicles. The identification of syd vesicle protein composition should contribute to define the mechanisms regulating axonal growth, guidance, and repair.

REFERENCES

1. Perlson, E., Jeong, G. B., Ross, J. L., Dixit, R., Wallace, K. E., Kalb, R. G., and Holzbaur, E. L. (2009) *J. Neurosci.* **29,** 9903–9917
2. Salinas, S., Bilsland, L. G., and Schiavo, G. (2008) *Curr. Opin. Cell Biol.* **20,** 445–453
3. Takamori, S., Holt, M., Stenius, K., Lemke, E. A., Grønborg, M., Riedel, D.,

Urlaub, H., Schenck, S., Brügger, B., Ringler, P., Müller, S. A., Rammner, B., Gräter, F., Hub, J. S., De Groot, B. L., Mieskes, G., Moriyama, Y., Klingauf, J., Grubmüller, H., Heuser, J., Wieland, F., and Jahn, R. (2006) *Cell* **127,** 831–846
4. Takamori, S., Riedel, D., and Jahn, R. (2000) *J. Neurosci.* **20,** 4904–4911
5. Burger, P. M., Mehl, E., Cameron, P. L., Maycox, P. R., Baumert, M., Lottspeich, F., De Camilli, P., and Jahn, R. (1989) *Neuron* **3,** 715–720
6. Morciano, M., Burré, J., Corvey, C., Karas, M., Zimmermann, H., and Volknandt, W. (2005) *J. Neurochem.* **95,** 1732–1745
7. Fischer von Mollard, G., Stahl, B., Walch-Solimena, C., Takei, K., Daniels, L., Khoklatchev, A., De Camilli, P., Südhof, T. C., and Jahn, R. (1994) *Eur. J. Cell Biol.* **65,** 319–326
8. Zhai, R. G., Vardinon-Friedman, H., Cases-Langhoff, C., Becker, B., Gundelfinger, E. D., Ziv, N. E., and Garner, C. C. (2001) *Neuron* **29,** 131–143
9. Delcroix, J. D., Valletta, J. S., Wu, C., Hunt, S. J., Kowal, A. S., and Mobley, W. C. (2003) *Neuron* **39,** 69–84
10. Cui, B., Wu, C., Chen, L., Ramirez, A., Bearer, E. L., Li, W. P., Mobley, W. C., and Chu, S. (2007) *Proc. Natl. Acad. Sci. U.S.A.* **104,** 13666–13671
11. Deinhardt, K., Salinas, S., Verastegui, C., Watson, R., Worth, D., Hanrahan, S., Bucci, C., and Schiavo, G. (2006) *Neuron* **52,** 293–305
12. Nielsen, E., Severin, F., Backer, J. M., Hyman, A. A., and Zerial, M. (1999) *Nat. Cell Biol.* **1,** 376–382
13. Bowman, A. B., Kamal, A., Ritchings, B. W., Philp, A. V., McGrail, M., Gindhart, J. G., and Goldstein, L. S. (2000) *Cell* **103,** 583–594
14. Ito, M., Yoshioka, K., Akechi, M., Yamashita, S., Takamatsu, N., Sugiyama, K., Hibi, M., Nakabeppu, Y., Shiba, T., and Yamamoto, K. I. (1999) *Mol. Cell. Biol.* **19,** 7539–7548
15. Kelkar, N., Gupta, S., Dickens, M., and Davis, R. J. (2000) *Mol. Cell. Biol.* **20,** 1030–1043
16. Cavalli, V., Kujala, P., Klumperman, J., and Goldstein, L. S. (2005) *J. Cell Biol.* **168,** 775–787
17. Kelkar, N., Delmotte, M. H., Weston, C. R., Barrett, T., Sheppard, B. J., Flavell, R. A., and Davis, R. J. (2003) *Proc. Natl. Acad. Sci. U.S.A.* **100,** 9843–9848
18. Ha, H. Y., Cho, I. H., Lee, K. W., Lee, K. W., Song, J. Y., Kim, K. S., Yu, Y. M., Lee, J. K., Song, J. S., Yang, S. D., Shin, H. S., and Han, P. L. (2005) *Dev. Biol.* **277,** 184–199
19. Abe, N., and Cavalli, V. (2008) *Curr. Opin. Neurobiol.* **18,** 276–283
20. Ambron, R. T., Zhang, X. P., Gunstream, J. D., Povelones, M., and Walters, E. T. (1996) *J. Neurosci.* **16,** 7469–7477
21. Hanz, S., and Fainzilber, M. (2006) *J. Neurochem.* **99,** 13–19
22. Rishal, I., and Fainzilber, M. (2009) *Exp. Neurol.*, in press
23. Perlson, E., Hanz, S., Ben-Yaakov, K., Segal-Ruder, Y., Seger, R., and Fainzilber, M. (2005) *Neuron* **45,** 715–726
24. Hanz, S., Perlson, E., Willis, D., Zheng, J. Q., Massarwa, R., Huerta, J. J., Koltzenburg, M., Kohler, M., van-Minnen, J., Twiss, J. L., and Fainzilber, M. (2003) *Neuron* **40,** 1095–1104
25. Willis, D., Li, K. W., Zheng, J. Q., Chang, J. H., Smit, A., Kelly, T., Merianda, T. T., Sylvester, J., van Minnen, J., and Twiss, J. L. (2005) *J. Neurosci.* **25,** 778–791
26. van Niekerk, E. A., Willis, D. E., Chang, J. H., Reumann, K., Heise, T., and Twiss, J. L. (2007) *Proc. Natl. Acad. Sci. U.S.A.* **104,** 12913–12918
27. Arantes, R. M., and Andrews, N. W. (2006) *J. Neurosci.* **26,** 4630–4637
28. Xia, C. H., Roberts, E. A., Her, L. S., Liu, X., Williams, D. S., Cleveland, D. W., and Goldstein, L. S. (2003) *J. Cell Biol.* **161,** 55–66
29. Huttner, W. B., Schiebler, W., Greengard, P., and De Camilli, P. (1983) *J. Cell Biol.* **96,** 1374–1388
30. Ogawa, S., Lozach, J., Jepsen, K., Sawka-Verhelle, D., Perissi, V., Sasik, R., Rose, D. W., Johnson, R. S., Rosenfeld, M. G., and Glass, C. K. (2004) *Proc. Natl. Acad. Sci. U.S.A.* **101,** 14461–14466
31. De Camilli, P., Harris, S. M., Jr., Huttner, W. B., and Greengard, P. (1983) *J. Cell Biol.* **96,** 1355–1373
32. Trischler, M., Stoorvogel, W., and Ullrich, O. (1999) *J. Cell Sci.* **112,** 4773–4783
33. Ikin, A. F., Annaert, W. G., Takei, K., De Camilli, P., Jahn, R., Greengard, P., and Buxbaum, J. D. (1996) *J. Biol. Chem.* **271,** 31783–31786
34. Yamazaki, H., Nakata, T., Okada, Y., and Hirokawa, N. (1995) *J. Cell Biol.* **130,** 1387–1399
35. Wang, Y., and Tang, B. L. (2006) *Mol. Membr. Biol.* **23,** 377–384
36. Zerial, M., and McBride, H. (2001) *Nat. Rev. Mol. Cell Biol.* **2,** 107–117
37. Chilcote, T. J., Galli, T., Mundigl, O., Edelmann, L., McPherson, P. S., Takei, K., and De Camilli, P. (1995) *J. Cell Biol.* **129,** 219–231
38. Miura, E., Fukaya, M., Sato, T., Sugihara, K., Asano, M., Yoshioka, K., and Watanabe, M. (2006) *J. Neurochem.* **97,** 1431–1446
39. Becker, E. B., and Bonni, A. (2006) *Neuron* **49,** 655–662
40. Montagnac, G., Sibarita, J. B., Loubéry, S., Daviet, L., Romao, M., Raposo, G., and Chavrier, P. (2009) *Curr. Biol.* **19,** 184–195
41. Ikonomov, O. C., Fligger, J., Sbrissa, D., Dondapati, R., Mlak, K., Deeb, R., and Shisheva, A. (2009) *J. Biol. Chem.* **284,** 3750–3761
42. Prekeris, R., Foletti, D. L., and Scheller, R. H. (1999) *J. Neurosci.* **19,** 10324–10337
43. Yap, C. C., Wisco, D., Kujala, P., Lasiecka, Z. M., Cannon, J. T., Chang, M. C., Hirling, H., Klumperman, J., and Winckler, B. (2008) *J. Cell Biol.* **180,** 827–842
44. McMahon, H. T., Ushkaryov, Y. A., Edelmann, L., Link, E., Binz, T., Niemann, H., Jahn, R., and Südhof, T. C. (1993) *Nature* **364,** 346–349
45. Ibáñez, C. F. (2007) *Trends Cell Biol.* **17,** 519–528
46. Schweizer, F. E., and Ryan, T. A. (2006) *Curr. Opin. Neurobiol.* **16,** 298–304
47. Hirling, H. (2009) *Neuroscience* **158,** 36–44
48. Nixon, R. A., and Cataldo, A. M. (1995) *Trends Neurosci.* **18,** 489–496
49. Parton, R. G., Simons, K., and Dotti, C. G. (1992) *J. Cell Biol.* **119,** 123–137
50. Lalli, G., and Schiavo, G. (2002) *J. Cell Biol.* **156,** 233–239
51. Idone, V., Tam, C., Goss, J. W., Toomre, D., Pypaert, M., and Andrews, N. W. (2008) *J. Cell Biol.* **180,** 905–914
52. Reddy, A., Caler, E. V., and Andrews, N. W. (2001) *Cell* **106,** 157–169
53. Altick, A. L., Baryshnikova, L. M., Vu, T. Q., and von Bartheld, C. S. (2009) *J. Comp. Neurol.* **514,** 641–657
54. Weible, M. W., 2nd, and Hendry, I. A. (2004) *J. Neurobiol.* **58,** 230–243
55. van der Goot, F. G., and Gruenberg, J. (2006) *Trends Cell Biol.* **16,** 514–521
56. Brown, H. M., Van Epps, H. A., Goncharov, A., Grant, B. D., and Jin, Y. (2009) *Dev. Neurobiol.* **69,** 174–190
57. Byrd, D. T., Kawasaki, M., Walcoff, M., Hisamoto, N., Matsumoto, K., and Jin, Y. (2001) *Neuron* **32,** 787–800
58. Sakamoto, R., Byrd, D. T., Brown, H. M., Hisamoto, N., Matsumoto, K., and Jin, Y. (2005) *Mol. Biol. Cell* **16,** 483–496
59. Ogura, K., Shirakawa, M., Barnes, T. M., Hekimi, S., and Ohshima, Y. (1997) *Genes Dev.* **11,** 1801–1811